Simulation Credibility Assessment Methodology with FPGA-based Hardware-in-the-loop Platform

Xunhua Dai, Chenxu Ke, Quan Quan and Kai-Yuan Cai

Abstract—Electronic control systems are becoming more and more complicated, which makes it difficult to test them sufficiently only through experiments. Simulation is an efficient way in the development and testing of complex electronic systems, but the simulation results are always doubtful by people due to the lack of credible simulation platforms and assessment methods. This paper proposes a credible simulation platform based on real-time FPGA-based hardware-in-the-loop (HIL) simulation, and then an assessment method is proposed to quantitatively assess its simulation credibility. By using the FPGA to simulate all sensor chips, the simulation platform can ensure that the tested electronic system maintains the same hardware and software operating environment in both simulations and experiments, which makes it possible to perform the same tests in the simulation platform and the real experiment to compare and analyze the simulation errors. Then, the testing methods and assessment indices are proposed to assess the simulation platform from various perspectives, such as performance, time-domain response, and frequency-domain response. These indices are all normalized to the same scale (from 0 to 1) and mapped to a uniform assessment criterion, which makes it convenient to compare and synthesize different assessment indices. Finally, an overall assessment index is proposed by combining all assessment indices obtained from different tests to assess the simulation credibility of the whole simulation platform. The simulation platform and the proposed assessment method are applied to a multicopter system, where the effectiveness and practicability are verified by simulations and experiments.

Index Terms—Hardware-in-the-loop (HIL), Simulation, Electronic control System, Credibility Assessment, FPGA.

I. INTRODUCTION

Currently, electronic control systems (e.g., autopilot systems of unmanned vehicles) are becoming more and more complicated, which makes it more and more difficult to test them sufficiently only through experiments. Therefore, simulation techniques, especially hardware-in-the-loop (HIL) simulations, are more and more widely used in the development and testing phases of complex electronic control systems, such as power systems [1], [2], aircraft systems [3], automotive systems [4], and robotic systems [5]. Although experiments are considered to be more trusted than simulation tests, for many high-complex electronic control systems (e.g., autopilot systems of unmanned aircraft), comprehensive experimental testing is usually high-cost, inefficient, dangerous and regulatory restricted [6]. With the ever-increasing safety requirements of electronic control systems, the experimental testing methods become increasingly inefficient in revealing potential safety issues and covering critical test cases. Besides, in experiments, the true states of a plant can only be estimated by external

measuring devices or onboard sensors whose measured results may be easily affected by the many uncontrollable factors, such as noise, vibration, temperature, and unexpected interference or failure. Instead, in simulations, the true states are known precisely, which makes it more efficient and accurate in assessing the performance and safety level of an electronic control system. However, the simulation credibility [7] is still the most concerned problem for people (e.g., users, companies, and certification authorities) to acknowledge that the simulation results can be as credible as real experiments.

According to [7], simulation credibility can be assessed both qualitatively and quantitatively. The former assesses the quality of simulation by professional engineers based on circumstantial evidence, which is simple but not convincing enough; the latter requires to quantify the simulation errors relative to real systems, which is convincing but usually difficult to implement. In practice, the qualitative assessment is widely adopted in simulation credibility analysis. For example, in [8], [9], the credibility of the HIL simulation platforms is assessed by qualitatively comparing the simulations results with experimental results from several aspects. Since there is no widely accepted index and standard for simulation credibility assessment, it is hard to quantitatively compare and assess different simulation platforms from an objective and comprehensive perspective. For the above concerns, a comprehensive survey for the verification and validation of simulation credibility is introduced in [10], where the following problems are revealed. (i) Traditional simulations are too separated from the actual hardware system, which makes it difficult to compare the simulation results with the experimental results. (ii) The simulation credibility is informal and not accurate enough because it is mainly assessed by the experience of engineers [11]. In summary, the simulation credibility should be ensured from two aspects. (i) The credibility of the simulation platform should be first guaranteed by maintaining the same hardware and software operating environment of the tested electronic control systems in both simulations and experiments. (ii) A qualitative credibility assessment method should be proposed to assess the simulation results from a more objective and comprehensive perspective.

Electronic control systems can usually be divided into the plant system and the control system. In software simulation, the plant simulation software runs on the same computer with the control algorithms, which is different from the real system whose algorithms usually run in specialized hardware. As a result, the software simulation results are usually considered to be less credible compared with experiments in real systems. Then, HIL simulation is proposed to increase the simulation credibility by using Real-Time (RT) simulation computers and

The authors are with School of Automation Science and Electrical Engineering, Beihang University, Beijing 100191, China.

real control system in simulations. However, limited by the performance of RT simulation computers, it is usually difficult for traditional RT simulation computers to simulate some sensors with high-speed communication interfaces or high-frequency analog circuits [12]. For example, a nanosecond-level RT update frequency is required to simulate the high-speed Serial Peripheral Interface (SPI) communication, which is a difficult task for traditional RT computers (model update frequency usually smaller 100kHz) with commercial Central Processing Units (CPUs) [13]. In recent years, the Field Programmable Gate Array (FPGA) [14] is becoming a standard component for RT simulation computers, and Commercial-Off-The-Shelf (COTS) RT simulation computers (such as RT-LAB and NI-PXI) start to have the ability to directly simulate electronic chips and circuits with a nanosecond-level RT update frequency [15], [16]. Based on this, FPGA-based HIL simulation platforms can simulate almost everything (including plant motion, environment conditions, sensor hardware, and interfaces) outside the control system. By using the same control system in both HIL simulations and experiments, the structure difference between simulation systems and real systems can be significantly controlled.

In [7], several assessment methods are proposed to assess simulation credibility, but these methods mainly focus on one specific feature instead of the whole system. Besides, many studies [8], [9] use the simulation errors (result error between simulation and experiment) as assessment indices to assess the simulation accuracy, but these indices are usually of a range from 0 to $+\infty$, which are not as convenient as normalized indices with a range from 0 to 1. Besides, different assessment indices may have different physics meaning, scales, and units, so it is difficult to combine different indices for comprehensively assessing the whole simulation system. For example, [17] proposes a cost function $J \in (0, +\infty]$ to assess the modeling accuracy by analyzing the Bode magnitude and phase information in the frequency domain. The cost function J is obtained by combining the magnitude error and the phase error (between simulations and experiments) with a constant scaling factor determined by human experience. One disadvantage of using constant factors to combining different indices with value range $(0, +\infty]$ is that some indices will be ignored when their orders of magnitudes are too different, which requires people to find appropriate scaling factors for specific systems. In summary, there is still a lack of practical and comprehensive simulation assessment methods widely recognized and accepted in the simulation filed.

The main work and contributions of this paper are as follows. (i) An FPGA-based HIL simulation platform is proposed to be able to simulate all situations as real experiments do and eliminate disturbance factors for simulation credibility assessments. (ii) Normalized assessment indices (the index range is from 0 to 1) are proposed and mapped into a uniform assessment criterion (e.g., a passing mark 0.6), which are practical and intuitive for comparison between different physical quantities. (iii) Multiple factors (including performance, time-domain response, and the frequency-domain response) are considered to assess the simulation credibility of the HIL platform comprehensively. (iv) An overall assessment index

is proposed by combining the above indices to assess the simulation credibility of the whole HIL simulation system. In the verification part, the HIL simulation platform is successfully applied to a quadcopter system, and its simulation results are compared with the experimental results to assess the simulation credibility with the proposed method. The experiments and comparisons demonstrate the effectiveness and practicability of the proposed platform and the credibility assessment method.

The rest of the paper is organized as follows. *Section* II gives a description of the FPGA-based HIL simulation platform and the testing methods for obtaining the simulation errors. Then, the simulation credibility assessment method is presented in *Section* III. In *Section* IV, the proposed platform and the assessment method are applied to a multicopter system to verify the proposed methods with experiments. *Section* V presents the conclusion and future work.

II. HIL PLATFORM AND TESTING METHOD

A. FPGA-based HIL Simulation

A modern complex electronic control system (e.g., autonomous vehicles and aircraft) can be divided into the plant system (e.g., the vehicle body and the actuators) and the control system (e.g., the autopilot system), where the control system is the most important component that determines the performance in normal situation and safety in failure situations. Fig. 1(a) presents the operating principle of a real electronic control system, where the plant motion information is sensed by sensors and then transmitted into the control system to acquire control commands for driving the actuators. In order to maximally maintain the system structure and operating environment as the real electronic control system, an FPGA-based HIL simulation method is proposed with the structure depicted in Fig. 1(b), where the sensors and communication interfaces are blocked and replaced by a model running in the FPGA to exchange the simulated sensor data and control signals with the control system. With comprehensively modeling all necessary elements (e.g., the plant system, sensors, environment, measuring noise, disturbances, and faults), the HIL simulation platform can theoretically simulate any situation as the electronic control system.
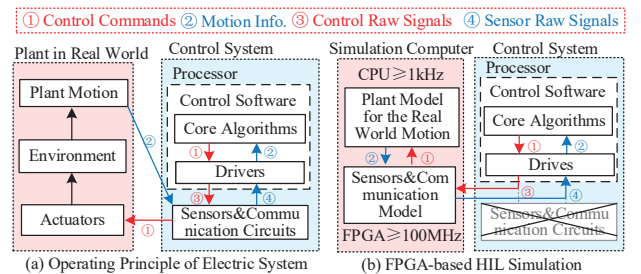

Fig. 1. Testing methods in real-world experiments and the FPGA-based HIL simulation platform.

B. Testing and Assessment Framework

As shown in Fig. 2, the most effective way to assess the simulation credibility is to input the same signals to both
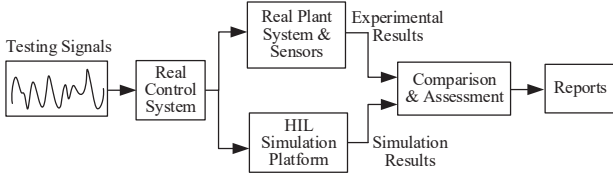
Fig. 2. Simulation validation testing structure.

(a) Step response performance parameters   (b) Time-domain testing results

Fig. 3. Typical simulation and experimental results.

the HIL simulation system and the real system to compare their result errors. The input signals should be selected from multiple aspects (including system performance, time-domain response, and frequency-domain response) to fully excite the system to reveal the system properties comprehensively. By using the same control system (see Fig. 2) in both simulations and experiments, the simulation errors caused by hardware and software differences of control systems can be controlled to the utmost extent, which significantly improves the credibility of the simulation platform compared with other simulation methods.

C. Assessment Index Normalization

The error e between simulation and experimental is the most important index to assess the simulation credibility. However, its value range $e \in [0, +\infty)$ is not suitable for comparison and assessment. In practice, an error threshold $\varepsilon > 0$ can be obtained from design experience or related standards to define the accepting error range $e \leq \varepsilon$ for assessment. Based on that, a normalization function is introduced here to map the error index $e \in [0, +\infty)$ to an assessment index $\eta \in (0, 1]$ with the error bound $e \leq \varepsilon$ corresponding to a desired passing mark $\eta \geq \eta_{\text{pass}}$ as

$$\eta \triangleq f_{\text{norm}}(e, \varepsilon) = \frac{K_e \cdot \varepsilon}{\sqrt{(K_e \cdot \varepsilon)^2 + e^2}} \quad (1)$$

where the coefficient $K_e \in \mathbb{R}^+$ is a scale factor to ensure $\eta_{\text{pass}} = f_{\text{norm}}(e = \varepsilon, \varepsilon)$, which gives

$$K_e = \frac{\eta_{\text{pass}}}{\sqrt{1 - \eta_{\text{pass}}^2}}. \quad (2)$$

Noteworthy, to accord with people's assessing habits, the passing mark η_{pass} can usually be selected as $\eta_{\text{pass}} \triangleq 0.6$ (or marked with 60%), which yields from (2) that $K_e = 0.75$. The physical meaning for the assessment index η is that: $\eta \to 0$ for worse simulation credibility, $\eta \to 1$ for better credibility, and $\eta = 0.6$ for a credibility passing line.

III. SIMULATION CREDIBILITY ASSESSMENT

The characteristics of an electronic control system can usually be described by many performance parameters, such as endurance, response delay, and maximum speed. Meanwhile, many testing results can also be summarized by several performance parameters, such as the percent overshoot σ_s, the settling time T_s of a step response curve presented in Fig. 3(a). In practice, comparing the performance parameters of the simulation system with the real system is the most commonly
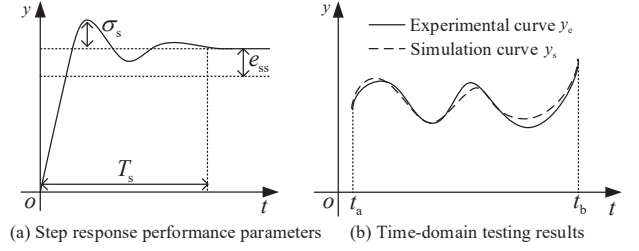
used way to assess simulation credibility, but it may ignore many important dynamic or frequency features. Thus, the time-domain testing and frequency-domain testing should also be considered in the simulation assessment method. This section will assess the simulation credibility of the whole simulation system by considering the above features comprehensively.

A. Performance Credibility

By applying direct measurement methods [18] or system identification methods [17] to the HIL simulation system and the real system presented in Fig. 2, the performance parameters can be obtained for the simulation system p_s and the real experimental system p_e, and the simulation error e_p is defined as

$$e_p \triangleq |p_e - p_s|. \quad (3)$$

As mentioned in (1), an error threshold $\varepsilon_p \in \mathbb{R}^+$ should be obtained from design experience or related standards for the assessment requirements. To simplify the selection process for ε_p and minimize the human subjectively, a dynamic selection method for ε_p is proposed in this paper as

$$\varepsilon_p = K_p \cdot |p_e|. \quad (4)$$

where $K_p \in \mathbb{R}^+$ is a percentage coefficient, and $K_p = 5\%$ is usually applicable for most situations. The expression of (4) indicates the threshold ε_p is dynamically adjusted with the detailed experimental value p_e. This is reasonable because a larger measured value usually has a larger error bound. The percentage coefficient K_p is also adjustable according to the actual situation. For example, a larger coefficient K_p should be selected when the disturbance or measuring errors are relatively large. Noteworthy, (4) may not apply to the situation $p_e = 0$ because $\varepsilon_p > 0$ must be satisfied for the following computation. In this case, other methods should be applied to determine ε_p, such as $\varepsilon_p = K_p \cdot |p_s|$.

Since $e_p \in [0, +\infty)$ is suitable for credibility assessment, the normalization function in (1) is applied to define the performance credibility index η_p as

$$\eta_p = f_{\text{norm}}(e_p, \varepsilon_p) = \frac{K_e \cdot \varepsilon_p}{\sqrt{(K_e \cdot \varepsilon_p)^2 + e_p^2}} \quad (5)$$

where, similar to (1), the range of η_p is $(0, 1]$ with a the passing mark $\eta_p \geq 0.6$ (corresponds to $e_p \leq \varepsilon_p$) to present the matching degree with the real system.

B. Time-domain Credibility

The time-domain testing results obtained from systems in Fig. 2 can be described by the data curves presented in Fig. 3(b), where $y_e(t)$ denotes the experimental curve, $y_s(t)$ denotes the simulation curve, and $t \in [t_a, t_b]$ denotes the tested interval. The time-domain credibility can be assessed by obtaining the average error between the simulation curves and the experimental curves. First, dividing the interval $[t_a, t_b]$ into n_t sample points as $t_1, t_2, \cdots, t_{n_t}$, the average error between the simulation curve and the experimental curve can be computed by

$$e_t = \sqrt{\frac{1}{n_t} \sum_1^{n_t} (y_e(t_i) - y_s(t_i))^2}. \tag{6}$$

Secondly, similar to (4), a feasible selection method for the error threshold ε_t is proposed as

$$\varepsilon_t = K_p \cdot \max_{1 \le i, j \le n_t} |y_e(t_i) - y_e(t_j)| \tag{7}$$

where K_p is a percentage coefficient as defined in (4). The expression of (7) indicates the maximum tolerable threshold ε_t is proportional to the maximum range of the experimental curve $y_e(t)$. Finally, according to (1), the normalized time-domain credibility index η_t is given by

$$\eta_t = f_{norm}(e_t, \varepsilon_t). \tag{8}$$

Noteworthy, the variable t for the curve functions $y_e(t)$ and $y_s(t)$ does not have to be time. Any measured curves (e.g., movement trajectories, motor throttle-speed curves, and air resistance curves) can be applied to assess the time-domain credibility η_t of the simulation systems. To reduce the calculation error, curve smoothing methods should be applied to (6) when the obtained curves are affected by disturbances or measuring noises. Besides, the time-domain index η_t is not suitable for assessing stochastic curves (e.g., noise signals and vibration signals), which can be assessed by the performance assessment index η_p with statistical parameters (e.g., mean value and variance).

C. Frequency-domain Credibility

1) Sweep-frequency Result Coherence: The frequency-domain testing should also be performed for systems in Fig. 2 to sufficiently excite the system characteristics within the frequency range of interest. First, according to [17], a coherence index η_{η_0} at the given frequency point f is necessary for evaluating the frequency-domain test results as

$$\eta_{co}(f) = \frac{\left| \hat{G}_{xy}(f) \right|^2}{\left| \hat{G}_{xx}(f) \right| \cdot \left| \hat{G}_{yy}(f) \right|} \tag{9}$$

where $\hat{G}_{xy}(f)$ is the cross-spectrum estimation of the input signal and the output signal at the frequency point f, $\hat{G}_{xx}(f)$ is the auto-spectrum estimation of the input signal, and $\hat{G}_{yy}(f)$ is the auto-spectrum estimation of the output signal [17, p. 30]. The range of the coherence index η_{co} is
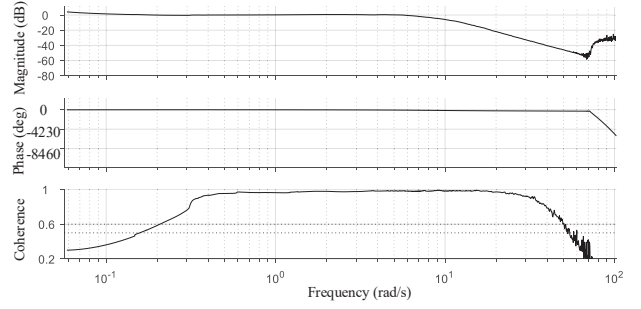

Fig. 4. Sweep frequency data processing results with the software CIFER®.

$(0, 1]$, and $\eta_{co} \to 1$ denotes the results obtained by frequency-domain testing are more accurate and credible. For the given frequency range of interest $f_{min} \le f \le f_{max}$, only when the following criterion is satisfied

$$\eta_{co}(f) \ge \varepsilon_{co}, \ f_a \le f \le f_b \tag{10}$$

then the frequency-domain testing results are considered accurate and credible for the following assessment process, where a threshold $\varepsilon_{co} = 0.6$ is recommended in [17, p. 38].

2) Simulation Errors in Magnitude and Phase Plots: The frequency-domain response of a system can be described by Bode plots, which include the magnitude plot and the phase plot. By performing sweep-frequency tests to the real system and the simulation system in Fig. 2, the magnitude and phase curves can be obtained by frequency-domain identification tools such as CIFER® [17] and MATLAB®. In this paper, the CIFER® software is applied to process the sweep-frequency testing results, and a demo of obtained results is depicted in Fig. 4.

Let $M_e(f)$ and $P_e(f)$ be the experimental magnitude and phase curves from the real system, and $M_s(f)$ and $P_s(f)$ be the simulated magnitude and phase curves from the simulation system. Then, by dividing the frequency interval $[f_a, f_b]$ to n_f sample points $f_1, f_2, \cdots f_{n_f}$, the average magnitude curve error e_{mag} and phase curve e_{pha} can be obtained as

$$e_{mag} = \sqrt{\frac{1}{n_f} \sum_1^{n_f} W_\gamma^2(f_i)(M_e(f_i) - M_s(f_i))^2} \tag{11}$$

$$e_{pha} = \sqrt{\frac{1}{n_f} \sum_1^{n_f} W_\gamma^2(f_i)(P_e(f_i) - P_s(f_i))^2} \tag{12}$$

where $W_\gamma(f) \in (0, 1]$ is a weighting function ($\eta_{co} \to 1 \Rightarrow W_\gamma \to 1$) to ensure the sample points f_i with higher coherence η_{co} have larger weight W_γ. Based on the research in [17, p. 280], the weighting function $W_\gamma(f)$ is given by

$$W_\gamma(f) = \frac{\left(1 - e^{-\eta_{co}(f)}\right)}{1 - e^{-1}} \tag{13}$$

which ensures the most effectively use of the testing data with different testing reliability. Noteworthy, $W_\gamma(f) \equiv 1$ can be applied to simplify the computational process of (11) and (12) when accuracy requirement is not too high.

3) Frequency-domain Assessment Index: Let $\varepsilon_{\text{mag}} \in \mathbb{R}^+$ and $\varepsilon_{\text{pha}} \in \mathbb{R}^+$ present the thresholds for the magnitude and phase average errors e_{mag} and e_{pha}, receptively. Similar to (7), the selection methods for ε_{mag} and ε_{pha} are given by

$$\varepsilon_{\text{mag}} = K_{\text{p}} \cdot \max_{1 \leq i,j \leqslant n_{\text{f}}} |M_{\text{e}}(f_i) - M_{\text{e}}(f_j)| \tag{14}$$

$$\varepsilon_{\text{pha}} = K_{\text{p}} \cdot \max_{1 \leq i,j \leqslant n_{\text{f}}} |P_{\text{e}}(f_i) - P_{\text{e}}(f_j)| \tag{15}$$

where K_{p} is a percentage coefficient as defined in (4).

Letting $\eta_{\text{mag}} \in (0,1]$ and $\eta_{\text{pha}} \in (0,1]$ present the model credibility in the magnitude aspect and phase aspect, their expressions can be obtained by (1) as

$$\begin{aligned} \eta_{\text{mag}} &= f_{\text{norm}}(e_{\text{mag}}, \varepsilon_{\text{mag}}) \\ \eta_{\text{pha}} &= f_{\text{norm}}(e_{\text{pha}}, \varepsilon_{\text{pha}}) \end{aligned} \tag{16}$$

Finally, the overall frequency-domain credibility index $\eta_{\text{f}} \in (0,1]$ is combined from (16) as

$$\eta_{\text{f}} = \sqrt{\frac{1}{2}\left(\eta_{\text{mag}}^2 + \eta_{\text{pha}}^2\right)} \tag{17}$$

where η_{f} is capable of combining the errors e_{mag} and e_{pha} at the same scale, and η_{f} is also normalized index with a passing mark 0.6 as (1).

D. Overall Simulation Credibility

Assuming that enough assessment tests (n_{p} performance parameter tests $\eta_{\text{p},i}$, n_{t} time-domain tests $\eta_{\text{t},i}$, and n_{f} frequency-domain tests $\eta_{\text{f},i}$) have been performed with the whole assessment indices for the performance credibility $\overline{\eta}_{\text{p}}$, the time-domain credibility $\overline{\eta}_{\text{t}}$, and the frequency-domain credibility $\overline{\eta}_{\text{f}}$ are given by

$$\overline{\eta}_{\text{p}} = \sqrt{\frac{1}{n_{\text{p}}}\sum_{i=1}^{n_{\text{p}}}\eta_{\text{p},i}^2}, \ \overline{\eta}_{\text{t}} = \sqrt{\frac{1}{n_{\text{t}}}\sum_{i=1}^{n_{\text{t}}}\eta_{\text{t},i}^2}, \ \overline{\eta}_{\text{f}} = \sqrt{\frac{1}{n_{\text{f}}}\sum_{i=1}^{n_{\text{f}}}\eta_{\text{f},i}^2}. \tag{18}$$

Then, the overall assessment index η_{all} for the whole system is given by

$$\eta_{\text{all}} = \sqrt{\alpha_{\text{p}} \cdot \overline{\eta}_{\text{p}}^2 + \alpha_{\text{t}} \cdot \overline{\eta}_{\text{t}}^2 + \alpha_{\text{f}} \cdot \overline{\eta}_{\text{f}}^2} \tag{19}$$

where $\alpha_{\text{p}}, \alpha_{\text{t}}, \alpha_{\text{f}} \in [0,1]$ are weighting factors with constraint $\alpha_{\text{p}} + \alpha_{\text{t}} + \alpha_{\text{f}} = 1$. The overall index η_{all} describes the average simulation credibility of a model from multiple assessment aspects, but it cannot describe the worst situation. For some safety-critical systems, the minimum index among all assessment indices is also very important for the worst credibility requirement. The minimum credibility index η_{min} can be computed by

$$\eta_{\text{min}} = \min_{i \leq n_{\text{p}}, j \leq n_{\text{t}}, k \leq n_{\text{f}}} \{\eta_{\text{p},i}, \ \eta_{\text{t},j}, \ \eta_{\text{f},k}\}. \tag{20}$$

In practice, a threshold ε_{min} should be given for η_{min} to describe the actual credibility requirement. For example, the threshold $\varepsilon_{\text{min}} = 90\%$ is selected for defining a high-credibility simulation model. If $\eta_{\text{min}} \geq \varepsilon_{\text{min}}$ is satisfied, then the overall assessment index η_{all} can be effective for assessing the simulation accuracy.
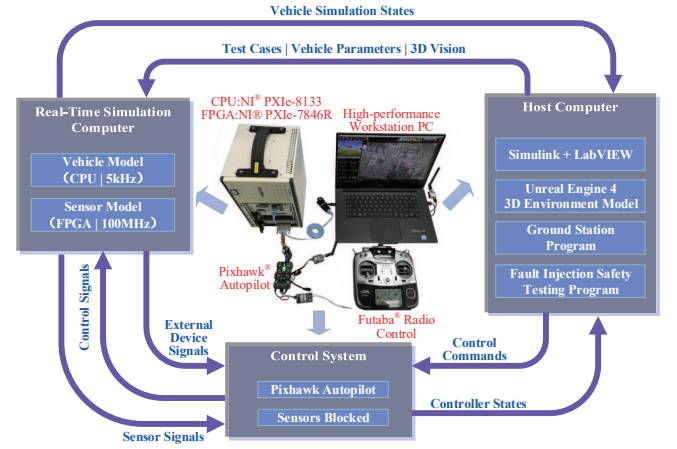

Fig. 5. Hardware composition of the real-time HIL simulation platform.

IV. VERIFICATION AND APPLICATION

In this section, an FPGA-based HIL simulation platform is first developed for a multicopter system. Then, its simulation credibility is assessed by the proposed assessment method.

A. HIL Simulation Platform

1) Hardware Composition: Based on the structure in Fig. 1(b), an FPGA-based HIL simulation platform is developed by the authors with the hardware component and connection relationship shown in Fig. 5. The simulation computer comes from National Instruments® (NI) with the CPU Module: PXIe-8133 (Intel Core I7 Processor, PharLap ETS Real-Time System) and FPGA I/O Module: PXIe-7846R. The host computer is a high-performance workstation PC with professional GPU to generate vision data for the simulation computer. The autopilot hardware system is the Pixhawk® autopilot, which is a popular open-source control system for small aircraft, vehicles, rovers, etc. All the onboard sensors (e.g., IMU, magnetometer, and barometer) and external sensors (e.g., GPS, accelerometer, rangefinder, and camera) of the Pixhawk® hardware have been blocked, and the sensor pins are reconnected to the FPGA I/Os to generate sensor signals (interfaces: SPI, PWM, I²C, UART, etc.) for the control system. On the simulation computer, the update frequency of the vehicle simulation model is up to 5 kHz and the update frequency of sensor simulation model is up to 100 MHz, which are fast enough for most small-scale electronic control systems. The communication between the host computer and the real-time simulation computer is realized by network cables with TCP and UDP protocols.

2) Experimental Setup: Based on the testing method in Fig. 2, a series of comparative experiments and simulations are performed to assess the simulation credibility of the HIL simulation platform in Fig. 5 with the proposed assessment method. The experimental setup is presented in Fig. 6, where an F450 quadcopter airframe (diagonal length: 450mm, vehicle weight: 1.4kg, propulsion system: DJI E310, battery: LiPo 3S 4000mAh) is selected as the tested system. The simulation model of the F450 quadcopter is developed in MATLAB®/Simulink [19], [20] and imported into the HIL

(a) Indoor test equipment for attitude response identification

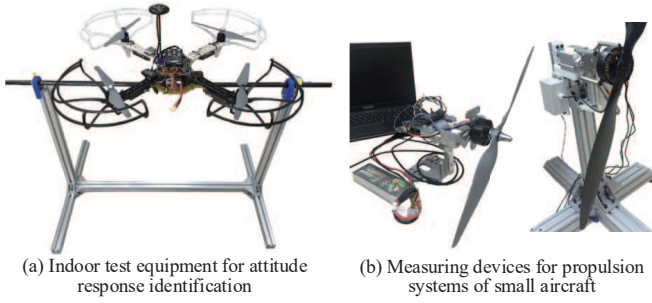(b) Measuring devices for propulsion systems of small aircraft

Fig. 6. Test equipment for simulation credibility assessment.

platform through code generation technique. In order to test the attitude dynamics of the quadcopter, an indoor test bench is developed with the setup shown in Fig. 6(a), where the quadcopter is fixed on a stiff stick (through the mass center) with high-precision bearings to minimize friction. The quadcopter is free to rotating along an axis smoothly, which makes it possible to perform sweep-frequency testing for the system identification of attitude dynamics. Fig. (b) presents the test benches to measure the propulsion system parameters of the quadcopter, where the detailed measuring methods can be found in [21], [22].

Since the controller parameters are associated the real aircraft and environment, if the real control system can control the simulated aircraft with similar flight performance as the real aircraft, the credibility of the simulation platform can be verified indirectly. According to our experiments, the Pixhawk® autopilot can control the simulated quadcopter model to finished normal flight tasks as a real quadcopter does, where a typical automatic flight mission test is presented in Fig. 7. Besides, the HIL simulation system is also applicable for automatic fault injection tests which are hard to achieve in real flight tests. A video (URL: https://youtu.be/D2hIIebVXsw) has been released to present the development process and testing cases for unmanned vehicle systems with the HIL simulation platform.

B. Experiments and Verification

1) Performance Credibility Assessment for Sensor Model: In order to verify the credibility of the sensor simulation methods, experiments and simulations are performed with the testing method presented in Fig. 2. The obtained results are presented in Fig. 8, where the simulated accelerometer and gyroscope are compared with the real sensor products. Figs. 8(a)(b) can verify that the sensor data generated by the HIL simulation system are highly coincident with the sensor data on real aircraft. To further assess the simulation effect from a quantitative view, the assessment method proposed in Section III is carried out to assess the simulation results presented in Fig. 8.

The performance credibility index η_p is selected here because the time-domain index η_t is not suitable for analyzing stochastic signals. The standard deviation σ is selected as the performance parameter in (3), where a threshold $\varepsilon_p \approx 10\% \cdot p_e$ is adopted according to the measuring uncertainty as
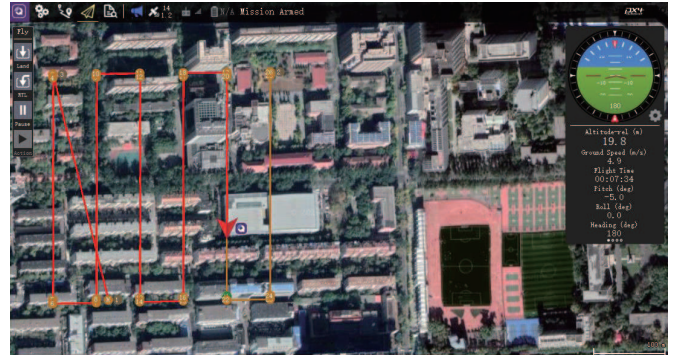
(a) QGC Ground Control Program for Automatic Mission Flight

(b) UE4 3D Flight Simulation Environment

(c) NI Simulation Computer & Pixhawk

Fig. 7. Automatic mission flight testing for F450 quadcopters. Figure (a) presents the real-time flight trajectory observed from the ground control station; (b) presents the high-fidelity 3D simulation scene where a chase viewpoint is presented for observing the vehicle attitude (the viewpoint is switchable to simulate vision from different onboard cameras); (c) presents the real product photo of the simulation computer and the Pixhawk® autopilot.

(a) Accelerometer noise&vibration test
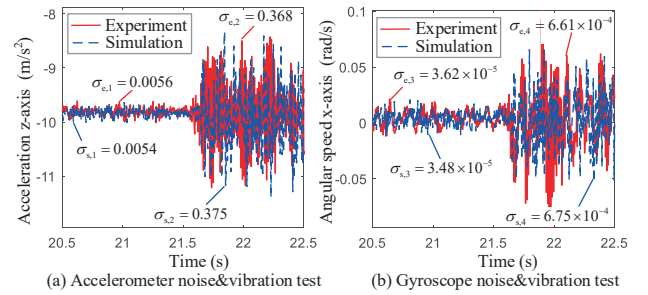
(b) Gyroscope noise&vibration test

Fig. 8. Sensor noise and vibration model verification test. The experiment data come from a real sensor product (MPU 6000), and the simulation data come from the simulated sensor model of the proposed real-time HIL platform. The motor speed is stepped from 0 to 50% to simulate the vibration on sensor data.

introduced in (4). The test results in Figs. 8(a)(b) are divided into four periods, and the simulation error for each period is obtained by $e_{p,i} = |\sigma_{e,i} - \sigma_{s,i}|$ according to (3). Then, the simulation credibility for each period $\eta_{p,i}$ can be obtained with the results listed in Table I. By combining the sensor credibility indices $\eta_{p,i}$ in Table I, the average simulation credibility is obtained by (18) as $\overline{\eta}_p = 94\%$. Since the obtained credibility index $\overline{\eta}_p = 94\%$ is far above the passing mark $\eta_{pass} = 60\%$, the simulation results can be considered accurate enough as a real sensor product.

2) Frequency-domain Credibility Assessment for Attitude Dynamics: In order to assess the frequency-domain credibility of the simulation platform, a series of sweeping frequency experiments are performed by using the test bench in Fig. 6(b). The input sweep signal and the attitude response output are depicted in Fig. 9(a), where the effective frequency testing range is $[f_a, f_b] = [0.25 \text{ rad/s}, 40 \text{ rad/s}]$. The testing data

TABLE I
ASSESSMENT INDICES OBTAINED FOR SENSOR DATA.

Test period	Parameter Error $e_{p,i}$	Threshold $\varepsilon_{p,i}$	Credibility Index $\eta_{p,i}$
Fig. 8(a): $t < 21.5$s	2×10^{-4}	6×10^{-4}	91.3%
Fig. 8(a): $t > 21.5$s	7×10^{-4}	4×10^{-3}	97.4%
Fig. 8(b): $t < 21.5$s	1.4×10^{-6}	4×10^{-6}	90.6%
Fig. 8(b): $t > 21.5$s	1.4×10^{-5}	7×10^{-5}	96.6%
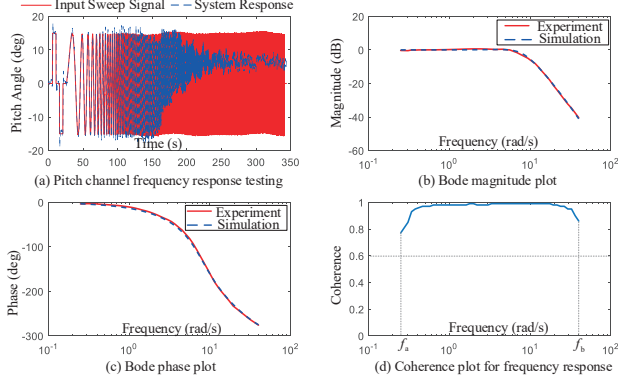
Fig. 9. Frequency-domain assessment for the simulation fidelity.

Fig. 10. Level flight results for simulation validation. The quadcopter is commanded to step from hovering mode to level flight mode.

in Fig. 9(a) is processed by the software CIFER® [17], and Figs. 9(b)(c)(d) present the obtained Bode's magnitude plot, Bode's phase plot, and coherence plot, respectively. Since the coherence curve $\eta_{co}(f)$ in Fig. 9(d) is far above the passing mark 0.6, the sweep testing results can be considered accurate and reliable according to the credibility criterion in (10). It can be observed from Figs. 9(b)(c)that the errors between the experiment curves and the simulation curves are very small in both magnitude and phase aspects, which verify the credibility of the simulation platform from the perspective of qualitative analysis.

In the following, the frequency-domain assessment index η_f in (17) will be applied to assess the simulation results from a quantitative perspective. For the magnitude curves in Figs. 9(b)(c), the magnitude credibility index is obtained by (11)-(16) as $\eta_{mag} = 97.3\%$ (the average error is $e_{mag} = 0.364$ and the threshold is $\varepsilon_{mag} = 2.05$); the phase credibility index is obtained as $\eta_{pha} = 97.6\%$ (the average error is $e_{pha} = 2.27$ and the threshold is $\varepsilon_{pha} = 13.6$). Finally, the frequency-domain fidelity index is obtained by (17) as $\eta_f = 97.63\%$, which indicates the pitch channel simulation model is of high-credibility relative to the real quadcopter.

For comparison, the sweep frequency results are also analyzed by CIFER® [17], and a cost function index $J \in [0, +\infty)$ for the modeling accuracy assessment is obtained as $J = 4.359$. Since there is no unified assessment standard, it is hard to describe the simulation credibility only with the cost index $J = 4.359$. According to the applications, the cost index J is more suitable for comparing the simulation results obtained from the same system, instead of comparing the simulation credibility among different systems. Moreover, the cost index J combines the magnitude error e_{magn} and phase error e_{pha} by using a constant scale factor k_J as $J^2 \propto (e_{magn}^2 + k_J \cdot e_{pha}^2)$, so one of the two errors will be ignored when their orders
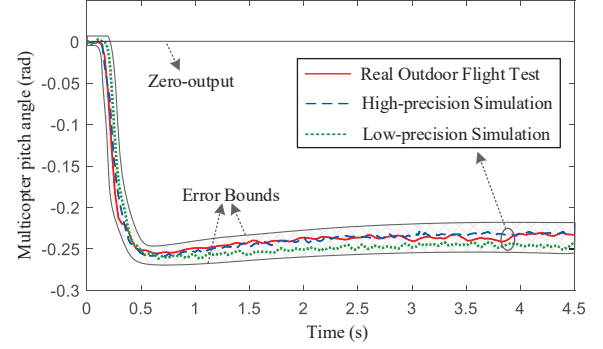
of magnitudes are too different (e.g., $e_{magn} \gg e_{pha}$, or $e_{magn} \ll e_{pha}$). In summary, compared the assessment index J in CIFER® with the proposed assessment index η_f is more intuitive and efficient for the simulation credibility assessment in the frequency domain.

3) Time-domain Credibility for Level Flight Test: For quantitative analysis, more outdoor flight tests are performed by the proposed HIL simulation platform with the typical testing results presented in Fig. 10. Since all the simulation factors (e.g., motion, aerodynamics, sensors, and disturbances) are involved in the level flight tests, the testing results can reflect the simulation credibility of the proposed platform in an overall and comprehensive way.

Three flight curves are presented in Fig. 10, where the real flight testing curve comes from the outdoor experiment, and the high-precision simulation curve and the high-precision simulation curve both come from the HIL simulation platform with different modeling precision. The high-precision simulation is performed with all model parameters being accurately measured by professional equipment or obtained by system identification methods; the low-precision simulation is from a simplified model with parameters obtained by analytical estimated. It can be observed from Fig. 10 that the high-precision simulation curve almost coincides with the real experimental curve, and the low-precision simulation curve is slightly different from the experimental curve, but the error is acceptable because it reveals most dynamic and aerodynamic characteristics of the quadcopter.

Quantitative analysis is carried out with the results listed in Table II to verify whether the time-domain assessment index $\eta_t \in (0, 1]$ can distinguish the slight simulation credibility difference. For comparison purposes, a zero-output curve (see Fig. 10) is also considered as a reference for the worst simulation accuracy case, and error bound curves (see Fig. 10) are obtained by (7) as $\varepsilon_t \approx 0.0175$. The results in Table II demonstrate that: (i) the assessment index is sensitive to reflect the difference among simulation platform with different modeling precision (the high-precision model $\eta_t = 94.4\%$ v.s. the low-precision model $\eta_t = 73.8\%$); (ii) the assessment index is capable of reflecting whether the accuracy satisfies the minimum threshold (the low-precision model $\eta_t = 73.8\% > 60\%$ indicates the simulation error is acceptable); (iii) the assessment index is sensitive to reflect the worst simulation

[2] A. Hadizadeh, M. Hashemi, M. Labbaf, and M. Parniani, "A matrix-inversion technique for FPGA-based real-time emt simulation of power converters," *IEEE Transactions on Industrial Electronics*, vol. 66, no. 2, pp. 1224–1234, 2019.

[3] C. Qi, F. Gao, X. Zhao, A. Ren, and Q. Wang, "A force compensation approach toward divergence of hardware-in-the-loop contact simulation system for damped elastic contact," *IEEE Transactions on Industrial Electronics*, vol. 64, no. 4, pp. 2933–2943, 2017.

[4] Y. Chen, S. Chen, T. Zhang, S. Zhang, and N. Zheng, "Autonomous vehicle testing and validation platform: Integrated simulation system with hardware in the loop," in *2018 IEEE Intelligent Vehicles Symposium (IV)*, 2018, pp. 949–956.

[5] I. Tejado, J. Serrano, E. Pérez, D. Torres, and B. M. Vinagre, "Low-cost hardware-in-the-loop testbed of a mobile robot to support learning in automatic control and robotics," *IFAC-PapersOnLine*, vol. 49, no. 6, pp. 242–247, 2016.

[6] D. Shi, X. Dai, X. Zhang, and Q. Quan, "A practical performance evaluation method for electric multicopters," *IEEE/ASME Transactions on Mechatronics*, vol. 22, no. 3, pp. 1337–1348, 2017.

[7] U. B. Mehta, D. R. Eklund, V. J. Romero, J. A. Pearce, and N. S. Keim, "Simulation credibility: Advances in verification, validation, and uncertainty quantification," NASA Ames Research Center, Moffett Field, CA United States, Tech. Rep. JANNAF/GL-2016-0001, Nov. 01, 2016.

[8] X. H. Mai, S. K. Kwak, J. H. Jung, and K. A. Kim, "Comprehensive electric-thermal photovoltaic modeling for power-hardware-in-the-loop simulation (PHILS) applications," *IEEE Transactions on Industrial Electronics*, vol. 64, no. 8, pp. 6255–6264, 2017.

[9] T. Roinila, T. Messo, R. Luhtala, R. Scharrenberg, E. C. De Jong, A. Fabian, and Y. Sun, "Hardware-in-the-loop methods for real-time frequency-response measurements of on-board power distribution systems," *IEEE Transactions on Industrial Electronics*, vol. 66, no. 7, pp. 5769–5777, 2019.

[10] R. G. Sargent and O. Balci, "History of verification and validation of simulation models," in *Proceedings of the 2017 Winter Simulation Conference*, ser. WSC '17. Piscataway, NJ, USA: IEEE Press, 2017, pp. 1–16.

[11] T. M. Morrison, P. Hariharan, C. M. Funkhouser, P. Afshari, M. Goodin, and M. Horner, "Assessing computational model credibility using a risk-based framework," *ASAIO Journal*, no. 4, pp. 349–360.

[12] O. Lucia, I. Urriza, L. A. Barragan, D. Navarro, O. Jimenez, and J. M. Burdio, "Real-time FPGA-based hardware-in-the-loop simulation test bench applied to multiple-output power converters," *IEEE Transactions on Industry Applications*, vol. 47, no. 2, pp. 853–860, 2010.

[13] H. Saad, T. Ould-Bachir, J. Mahseredjian, C. Dufour, S. Dennetiere, and S. Nguefeu, "Real-time simulation of MMCs using CPU and FPGA," *IEEE Transactions on Power Electronics*, vol. 30, no. 1, pp. 259–267, 2015.

[14] M. Matar and R. Iravani, "FPGA implementation of the power electronic converter model for real-time simulation of electromagnetic transients," *IEEE Transactions on Power Delivery*, vol. 25, no. 2, pp. 852–860, 2010.

[15] S. Mikkili, A. K. Panda, and J. Prattipati, "Review of real-time simulator and the steps involved for implementation of a model from MAT-LAB/SIMULINK to real-time," *Journal of The Institution of Engineers (India): Series B*, vol. 96, no. 2, pp. 179–196, 2015.

[16] S. S. Noureen, V. Roy, and S. B. Bayne, "An overall study of a real-time simulator and application of RT-LAB using MATLAB simpower-systems," in *2017 IEEE Green Energy and Smart Systems Conference*, 2018, pp. 1–5.

[17] R. K. Remple and M. B. Tischler, *Aircraft and rotorcraft system identification: engineering methods with flight-test examples*. American Institute of Aeronautics and Astronautics, 2006.

[18] Q. Quan, *Introduction to Multicopter Design and Control*. Springer, Singapore, 2017.

[19] B. L. Stevens and F. L. Lewis, *Aircraft Control and Simulation 2nd Edition*. Wiley, New Jersey, 2004.

[20] I. MathWorks, "Quadcopter flight simulation model - mambo," https://ww2.mathworks.cn/help/aeroblks/quadcopter-project.html, Accessed April 17, 2019.

[21] X. Dai, Q. Quan, J. Ren, and K.-Y. Cai, "An analytical design optimization method for electric propulsion systems of multicopter UAVs with desired hovering endurance," *IEEE/ASME Transactions on Mechatronics*, vol. 24, no. 1, pp. 228–239, 2019.

[22] X. Dai, Q. Quan, J. Ren, and C. Kai-Yuan, "Efficiency optimization and component selection for propulsion systems of electric multicopters," *IEEE Transactions on Industrial Electronics*, vol. 66, no. 10, pp. 7800–7809, 2019.

TABLE II
SIMULATION ASSESSMENT FOR MODELS WITH DIFFERENT ACCURACY

Curve Type	Mean Error e_t	Error Threshold ε_t	Assessment Index η_t
Real Flight	0	0.0175	100%
High-precision	0.0046	0.0175	94.4%
Low-precision	0.012	0.0175	73.8%
Error Bounds	0.0175	0.0175	60.0%
Zero-output	0.231	0.0175	1.75%

credibility (the zero-output curve $\eta_t = 1.75\% \to 0$).

4) Overall Simulation Credibility Assessment: With the above testing results, according to the computing expression in (18), the whole performance credibility is obtained as $\overline{\eta}_p = 94.0\%$, the whole frequency-domain credibility is obtained as $\overline{\eta}_f = 97.63\%$, and the whole time-domain credibility is obtained as $\overline{\eta}_t = 94.4\%$. Since the frequency-domain characteristic is usually more important for assessing a dynamic system, by selecting weight factors $\{\alpha_p, \alpha_t, \alpha_f\}$ as $\{0.3, 0.3, 0.4\}$, the overall simulation credibility η_{all} can be obtained by (19) as $\eta_{all} = 95.36\%$. Meanwhile, the minimum simulation credibility can be obtained by (20) as $\eta_{min} = 90.6\%$. Since only several testing results are presented in this section, the obtained indices η_{all} and η_{min} may be not comprehensive and representative enough. With more testing results are considered from different angles, the obtained indices η_{all} and η_{min} can become very comprehensive and representative to assess the simulation credibility of the whole HIL system. On the other hand, these assessment indices can help designers to find out the weak points of the simulation models to continually improve the simulation credibility.

V. CONCLUSION

All the above analyses demonstrate that (i) the proposed modeling method with the FPGA-based HIL simulation system is capable of simulating the vehicle characteristics as realistic as real vehicle systems; (ii) the proposed simulation credibility assessment method is efficient and practical in assessing the simulation credibility of simulation systems. Since all proposed assessment indices are normalized to 0 to 1 and scaled to the same passing mark 0.6, we can compare and combine different system characteristics within a unified assessment framework. The simulation credibility assessment is important in the verification and validation of the simulation platform compared with the real system, which provides the basis for applying the simulation testing results to the future safety assessment and certification frameworks, such as the airworthiness of unmanned aircraft systems. Based on the proposed platform and assessment method, more efficient and comprehensive automatic testing and assessment methods will be studied in the future for electronic systems to increase their safety and reliability levels.

REFERENCES

[1] C. Mao, F. Leng, J. Li, S. Zhang, L. Zhang, R. Mo, D. Wang, J. Zeng, X. Chen, R. An, and Y. Zhao, "A 400-V/50-kVA digital-physical hybrid real-time simulation platform for power systems," *IEEE Transactions on Industrial Electronics*, vol. 65, no. 5, pp. 3666–3676, 2018.